PERGAMON

International Journal of Heat and Mass Transfer 45 (2002) 1345–1352

International Journal of HEAT and MASS TRANSFER

www.elsevier.com/locate/ijhmt

Unsteady mixed convection flow in the stagnation region of a heated vertical plate due to impulsive motion

Rajeswari Seshadri [a], Nalini Sreeshylan [b], G. Nath [c,*]

[a] *Fluid Dynamics Unit, Jawaharlal Nehru Centre for Advanced Scientific Research, Bangalore 560 064, India*
[b] *Department of Mathematics, Indian Institute of Science, Bangalore 560 012, India*
[c] *B-20, Mahadeo Nagar Colony, Sarang Talab, P.O. Tapovan Ashram, Via Saranath, Varanasi, UP 221 007, India*

Received 14 February 2000

Abstract

The unsteady mixed convection in the stagnation flow on a heated vertical plate is studied where the unsteadiness is caused by the impulsive motion of the free stream velocity and by sudden increase in the surface temperature (heat flux). The short time as well as the long time solutions are included in the analysis. Both prescribed surface temperature and prescribed surface heat flux conditions are considered. The partial differential equations governing the flow and the heat transfer have been solved numerically using an implicit finite difference scheme. Also, the asymptotic behaviour of the solution for large value of the independent variable is examined when the flow becomes steady. There is a smooth transition from the small-time solution to the large-time solution. The surface shear stress and the heat transfer increase with time and buoyancy parameter. The heat transfer increases with the Prandtl number, but the surface shear stress decreases.

1. Introduction

The combined forced and free convection flow (mixed convection flow) is encountered in many technical and industrial applications which include solar central receivers exposed to wind currents, electronic devices cooled by fans, nuclear reactors cooled during emergency shutdown and heat exchangers placed in a low-velocity-environment. The two-dimensional stagnation flow in a forced convection refers to the flow in the vicinity of a stagnation line that results from a two-dimensional flow impinging on a surface at right angles and flowing there after symmetrically about the stagnation line. Hiemenz [1] studied the two-dimensional stagnation flow and Eckert [2] considered the corresponding heat transfer problem. The mixed convection in stagnation flow is important when the buoyancy forces due to the temperature difference between the surface and the free stream become large. Consequently, both the flow and thermal fields are significantly affected by the buoyancy forces. Ramachandran et al. [3] have investigated the mixed convection flow in the stagnation region of a vertical plate. The above studies deal with steady flows. In several problems the flow may be unsteady which might be caused by the change in the free stream velocity or in the surface temperature (surface heat flux) or in both.

When there is an impulsive change in the velocity field, the inviscid flow is developed instantaneously, but the flow in the viscous layer near the wall is developed slowly which becomes fully developed steady flow after sometime. For small time the flow is dominated by the viscous forces and the unsteady acceleration, but for large time it is dominated by the viscous forces, the pressure gradient and the convective acceleration. For small time the flow is generally independent of the conditions far upstream and at the leading edge or at the stagnation point and for large time the flow depends on these conditions. The mathematical problem for short time is governed by the Rayleigh type of equation and for large time by the Falkner–Skan type of equation.

The boundary layer flow development of a viscous fluid on a semi-infinite flat plate due to the impulsive

* Corresponding author.

0017-9310/02/$ - see front matter
PII: S0017-9310(01)00228-9

Nomenclature

a, b, c	constants
A_1, A_2, A_3	arbitrary constants
c_0, c_1, c_2, c_3	constants
c_f	skin friction coefficient
f	dimensionless stream function
g	gravitational acceleration
Gr_x, Gr_x^*	Grashof numbers for the prescribed surface temperature (PST) and the prescribed heat flux (PHF) cases, respectively.
k	thermal conductivity
m, n	constants
Nu	Nusselt number
Pr	Prandtl number
q_w	surface heat transfer
Re_x	Reynolds number
s_1, s_2, s_3, s_4	constants
t, t^*	dimensional and dimensionless times, respectively
T	temperature
u, v	velocity components along x and y directions, respectively
x, y	distances along and normal to the surface

Greek symbols

α	thermal diffusivity
β	coefficient of volumetric thermal expansion
β_1	constant
η	pseudo-similarity variable
θ	dimensionless temperature
λ_1, λ_2	buoyancy parameters for PST and PHF cases, respectively
μ	coefficient of viscosity
v	kinematic viscosity
ξ	dimensionless time

Subscripts

e, w, ∞	conditions at the edge of the boundary layer, at the surface, and in the free stream, respectively.
t, x, y	derivatives with respect to t, x and y, respectively

Superscript

$'$	denotes derivative with respect to η

motion of the free stream has been investigated by Stewartson [4,5], Hall [6], Dennis [7] and Watkins [8]. The corresponding problem over a wedge has been studied by Smith [9], Nanbu [10] and Williams and Rhyne [11].

Ece [12] has studied the flow development of the laminar boundary layer on an impulsively started translating and spinning rotational symmetric body, and the temporal development of the thermal boundary layer has been considered by Ozturk and Ece [13]. In both cases, the series solutions were obtained. Kumari [14] has examined the temporal development of momentum and thermal boundary layers on an impulsively started wedge with a magnetic filed and has obtained the solution numerically starting from the initial steady-state to the final steady-state.

Brown and Riley [15] have presented an analysis that covers three distinct phases in the temporal development of the free convection flow past a suddenly heated semi-infinite vertical plate. The unsteadiness in the flow field arises due to the step-change in wall temperature. In the initial stage one-dimensional flow describes the flow and a local solution describes the early stage of the departure from this. Finally, an asymptotic solution describes the manner in which the final steady-state is reached. Ingham [16] has considered essentially the same problem as that of Brown and Riley [15], but instead of taking the step-change in wall temperature, the wall temperature T_∞ is suddenly raised to $T_w = T_\infty + Ax^m$, where A is a positive constant, m is a constant and x is the distance measured from the leading edge of the plate. Both numerical and asymptotic solutions were obtained. It is found that the numerical solutions match the large- and small-time asymptotic solutions when the temperature increases along the length of the plate. However, no matching of these asymptotic solutions is found when the wall temperature decreases along the plate.

The mixed convection flow at a two-dimensional stagnation point on a heated horizontal boundary was investigated by Amin and Riley [17]. The forced flow is a stagnation point flow and the free convection part is due to a pressure gradient that is induced by temperature variations along the boundary. They have identified situations in which a steady flow can be maintained.

The aim of this analysis is to study the development of flow and heat transfer in the stagnation flow on a heated vertical plate in the presence of buoyancy forces. The unsteadiness in the flow field is caused by impulsively creating motion in the free stream and at the same time suddenly raising the surface temperature (heat flux) above its surroundings. The problem is formulated in such a way that at $t = 0$ it is represented by the Rayleigh type of equation and for $t \to \infty$ it is represented by the Hiemenz type of equation. The partial differential

equations governing the flow and the heat transfer have been solved numerically using the implicit finite-difference scheme [18]. Particular cases of the present results are compared with those of Ramachandran et al. [3].

2. Analysis

Let us consider a semi-infinite vertical plate which is placed in an ambient fluid with uniform temperature T_∞. At $t = 0$ the ambient fluid is impulsively moved with a velocity u_e and at the same time the surface temperature or heat flux is suddenly raised. Fig. 1 shows a flow field over a heated vertical surface where the upper half of the flow field is assisted by the buoyancy force, but the lower part is opposed by the buoyancy force. The reverse trend appears if the plate is cooled below. The results presented here are valid for both cases. The surface of the plate is assumed to have an arbitrary temperature or it is subjected to an arbitrary heat flux. Under the above assumptions along with Boussinesq approximation, the unsteady laminar boundary layer equations governing the mixed convection flow are given by [3]

$$u_x + v_y = 0, \tag{1}$$

$$u_t + uu_x + vu_y = u_e(u_e)_x + vu_{yy} + g\beta(T - T_\infty), \tag{2}$$

$$T_t + uT_x + vT_y = \alpha T_{yy}. \tag{3}$$

The initial conditions are

$$u(x,y) = v(x,y) = 0, \quad T(x,y) = T_\infty \quad \text{for } t < 0. \tag{4}$$

The boundary conditions for $t \geqslant 0$ are

$$u(x,0) = v(x,0) = 0, \quad u(x,\infty) = u_e = ax, \ a > 0,$$
$$T(x,\infty) = T_\infty, \quad T(x,0) = T_w(x) = bx^n, \ b > 0, \ n \geqslant 0$$
for prescribed surface temperature (PST case),
$$-K\frac{\partial T(x,0)}{\partial y} = q_w(x) = cx^n, \ c > 0$$
for prescribed surface heat flux (PHF case). (5)

The index $n = 0$ for constant surface temperature (heat flux) and $n = 1$ for linear surface temperature (heat flux).

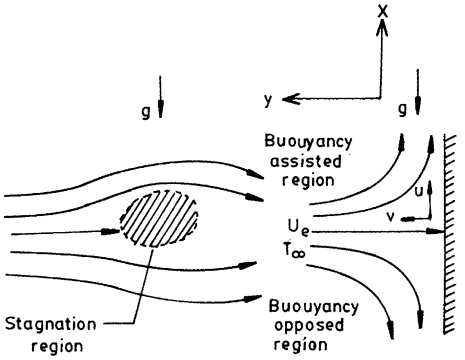

Fig. 1. The flow model and the coordinate system.

It may be remarked that we encounter certain difficulties in formulating the problem of boundary layer development due to the impulsive motion. For small-time solution we can use the scale $R = y/(vt)^{1/2}$, $t^* = u_e t/x$ and for large-time solution we can use the scale $\eta = y(u_e/vx)^{1/2}$, $t^* = u_e t/x$. If the problem is formulated in (R, t^*) system, the short-time solution fits in properly, but the large-time solution does not fit. This implies that we have to find a scaling of the y-coordinate which behaves like $y/(vt)^{1/2}$ for small time and as $y(u_e/vx)^{1/2}$ for large time. Further it is convenient to choose time scale ξ so that the region of time integration may become finite. Such transformations have been found by Williams and Rhyne [11] and they are given by

$$\eta = (a/v)^{1/2} y\xi^{-1/2}, \quad \xi = 1 - \exp(-t^*),$$
$$t^* = at, \ a > 0, \quad u(x,y,t) = axf'(\eta,\xi),$$
$$v(x,y,t) = -(av)^{1/2}\xi^{1/2} f(\eta,\xi),$$
$$T(x,y,t) = T_\infty + (T_w - T_\infty)\theta(\eta,\xi) \quad \text{(PST case)},$$
$$T(x,y,t) = T_\infty + (a/v)^{-1/2}(q_w/k)\theta(\eta,\xi) \quad \text{(PHF case)},$$
$$Pr = v/\alpha, \quad \lambda_1 = Gr_x/Re_x^2, \quad Gr_x = g\beta(T_w - T_\infty)x^3/v^2,$$
$$Re_x = ax^2/v, \quad \lambda_2 = Gr_x^*/Re_x^{5/2}, \quad Gr_x^* = g\beta q_w x^4/kv^2. \tag{6}$$

Using (6) in (1)–(3), we find that (1) is identically satisfied and (2) and (3) reduce to

$$f''' + 2^{-1}\eta(1-\xi)f'' + \xi ff'' + \xi(1 - f'^2) + \lambda\xi\theta = \xi(1-\xi)\frac{\partial f'}{\partial \xi}, \tag{7}$$

$$\theta'' + 2^{-1}Pr\eta(1-\xi)\theta' + Pr\xi(f\theta' - nf'\theta) = Pr\xi(1-\xi)\frac{\partial \theta'}{\partial \xi}, \tag{8}$$

where $\lambda = \lambda_1$ for the PST case and $\lambda = \lambda_2$ for the PHF case. Also $\lambda_1(\lambda_2) > 0$ for the buoyancy assisting flow and $\lambda_1(\lambda_2) < 0$ for the buoyancy opposing flow. The boundary conditions (5) reduce to

$$f(0,\xi) = f'(0,\xi) = 0, \quad f'(\infty,\xi) = 1,$$
$$\theta(\infty,\xi) = 0, \quad \theta(0,\xi) = 1 \text{ (PST case)}, \tag{9}$$
$$\theta'(0,\xi) = -1 \text{ (PHF case)}.$$

It may be noted that the buoyancy parameters λ_1 and λ_2 are the functions of streamwise distance x unless the surface temperature $(T_w - T_\infty)$ and the surface heat flux (q_w) vary linearly with x (i.e., $n = 1$). For $n = 1$, λ_1 and λ_2 are constants. In particular, if $b = c = g\beta a^2$, then $\lambda_1 = \lambda_2 = 1$. Hence for the self-similar solution both $T_w - T_\infty$ and q_w should vary linearly with x (i.e., $n = 1$). For $n \neq 1$, the equations are locally self-similar.

Eqs. (7) and (8) are coupled nonlinear parabolic partial differential equations, but for $\xi = 0, (t^* = 0)$ and $\xi = 1 (t^* \to \infty)$ they reduce to ordinary differential equations. For $\xi = 0$, (7) and (8) reduce to

$$f''' + 2^{-1}\eta f'' = 0, \tag{10}$$

$$\theta'' + 2^{-1}Pr\eta\theta' = 0. \tag{11}$$

For $\xi = 1$, (7) and (8) reduce to

$$f''' + ff'' + 1 - f'^2 + \lambda\theta = 0. \tag{12}$$

$$\theta'' + Pr(f\theta' - nf'\theta) = 0. \tag{13}$$

The boundary conditions for (10)–(13) are

$$\begin{aligned} &f(0) = f'(0) = 0, \quad f'(\infty) = 1, \quad \theta(\infty) = 0, \\ &\theta(0) = 1 \ \text{(PST case)}, \quad \theta'(0) = -1 \ \text{(PHF case)}. \end{aligned} \tag{14}$$

Eqs. (10) and (11) are uncoupled linear equations and (12) and (13) are coupled nonlinear equations. Eqs. (10) and (11) under conditions (14) admit closed form solutions which are given by

$$\begin{aligned} &f = \eta\,\mathrm{erf}(\eta/2) - (\pi)^{-1/2}[1 - \exp(-\eta^2/4)], \\ &\theta = \mathrm{erfc}(Pr^{1/2}\eta/2) \quad \text{(PST case)}, \\ &\theta = (\Pi/Pr)^{1/2}\mathrm{erfc}(Pr^{1/2}\eta/2) \quad \text{(PHF case)}. \end{aligned} \tag{15a}$$

Hence

$$f''(0) = (\Pi)^{-1/2}, \quad \theta'(0) = -(Pr/\Pi)^{1/2}. \tag{15b}$$

Eqs. (12) and (13) do not admit closed form solutions. Eqs. (7) and (8) under conditions (9) for $\xi = 1$ (steady case) are identical to those of Ramachandran et al. [3]. Also (7) under conditions (9) for $\lambda = 0$ (forced convection flow) is the same as that of Williams and Rhyne [11] if we put $m = 1$ in their equation.

For prescribed surface temperature or heat flux, the skin friction coefficient on the surface can be expressed as

$$\begin{aligned} c_f &= 2\mu\left(\frac{\partial u}{\partial y}\right)_{y=0} \Big/ \rho u_e^2 \\ &= 2\xi^{-1/2}Re_x^{-1/2}f''(\xi,0), \quad \xi > 0. \end{aligned} \tag{16a}$$

Similarly, the heat transfer coefficient in terms of the Nusselt number for the PST case can be written as

$$\begin{aligned} Nu &= \left(\frac{\partial T}{\partial y}\right)_{y=0} x \Big/ (T_w - T_\infty) \\ &= -Re_x^{1/2}\xi^{-1/2}\theta''(\xi,0), \quad \xi > 0. \end{aligned} \tag{16b}$$

For the PHF case, the Nusselt number can be expressed as

$$Nu = Re_x^{1/2}\xi^{-1/2}/\theta(\xi,0), \quad \xi > 0. \tag{16c}$$

3. Asymptotic solution

In this section, we examine the asymptotic behaviour of the solutions of (12) and (13) under conditions (14) for large $\eta(\eta \to \infty)$. As $\eta \to \infty$, $f' \to 1$, $\theta \to 0$. Hence we set

$$f = \eta - \beta_1 + f_1, \quad \theta = \theta_1, \quad \beta_1 = \lim_{\eta\to\infty}(\eta - f), \tag{17}$$

where f_1 and θ_1 are small so that their squares and products can be neglected. Using (17) in (12) and (13), we get

$$f_1''' + (\eta - \beta_1)f_1'' - 2f_1' + \lambda\theta_1 = 0, \tag{18}$$

$$\theta_1'' + Pr(\eta - \beta_1)\theta_1' - n\theta_1 = 0. \tag{19}$$

The boundary conditions on f_1 and θ_1 as $\eta \to \infty$ are given by

$$f_1 = f_1' = \theta_1 = 0 \text{ as } \eta \to \infty. \tag{20}$$

The solution of (18) and (19) under conditions (20) can be expressed in terms of parabolic cylinder function [19]

$$\begin{aligned} \theta_1 &= A_1 \exp\left[-(Pr+1)Pr\xi^2/4\right](Pr\xi)^{-m} \\ &\quad \times \left[1 - \frac{m(m+1)}{2(Pr\xi)^2} + O(\xi^{-4})\right], \end{aligned} \tag{21a}$$

$$\begin{aligned} f_1' &= A_2 \exp(-\xi^2/2)\xi^{-3}\left[1 - 6\xi^{-2} + O(\xi^{-4})\right] \\ &\quad + A_1\lambda \exp\left[-(Pr+1)Pr\xi^2/4\right](Pr\xi)^{-m} \\ &\quad \times \left[c_0 + c_1(Pr\xi)^{-2} + O(\xi^{-4})\right], \end{aligned} \tag{21b}$$

where

$$\begin{aligned} &\xi = \eta - \beta_1, \quad m = (n + 2^{-1})Pr + 2^{-1}, \\ &c_0 = \left[2^{-1}m(m+1)s_2 + s_4\right]/(s_2s_3 - s_1s_4), \\ &c_1 = \left[2^{-1}m(m+1)s_1 + s_3\right]/(s_1s_4 - s_2s_3), \\ &s_1 = 2^{-1}[(2m-1)Pr(Pr+1) - (m+2)], \\ &s_2 = 2^{-2}Pr^{-1}(Pr+1)[Pr(Pr+1) - 2], \\ &s_3 = m(m+1)Pr^2, \\ &s_4 = 2^{-1}(2m+3)Pr(Pr+1) - (m+4). \end{aligned} \tag{21c, 21d}$$

For $n = 0$ (constant surface temperature or heat flux)

$$\begin{aligned} \theta_1 &= -A_3(Pr\xi)^{-1}\exp(-Pr\xi^2/2) \\ &\quad \times \left[1 + (Pr\xi^2)^{-1} + O(\xi^{-4})\right], \end{aligned} \tag{22a}$$

$$\begin{aligned} f_1' &= A_2 \exp(-\xi^2/2)\xi^{-3}\left[1 - 6\xi^{-2} + O(\xi^{-4})\right] \\ &\quad + A_3\lambda\exp(-Pr\xi^2/2) \\ &\quad \times \left[c_2(Pr\xi)^{-1} + c_3(Pr^2\xi^3)^{-1} + O(\xi^{-5})\right], \end{aligned} \tag{22b}$$

where

$$\begin{aligned} &c_2 = (3Pr+1)/[Pr(3Pr-5)], \\ &c_3 = -(3Pr-1)/[(Pr-1)(3Pr-5)]; \\ &Pr \neq 1 \text{ and } 5/3. \end{aligned} \tag{22c}$$

It is evident from the above equations that f_1' and θ_1 tend to zero in an exponential manner as $\eta \to \infty$. Hence f' and θ tend to 1 and 0, respectively, as $\eta \to \infty$.

4. Method of solution

Eqs. (7) and (8) under conditions (9)–(13) are solved numerically using an implicit finite-difference scheme similar to that of Blottner [18]. The first-order derivatives with respect to ξ are replaced by two-point backward difference formulae of the form

$$\frac{\partial S}{\partial \xi} = (S_{m,n} - S_{m-1,n})/\Delta\xi, \tag{23}$$

where S represents any dependent variable and m and n are the node locations along ξ and η directions, respectively. First the third-order differential equation (7) is converted into second-order equation by substituting $f' = h$. The second-order equation for h is descretized using three-point central difference formulae while all first-order differential equations are descretized by using the trapezoidal rule. At each line of constant ξ, a system of algebraic equations is obtained. The nonlinear terms are evaluated at the previous iteration and the algebraic equations are solved iteratively by using the well known Thomas algorithm (see Blottner [18]). The same procedure is repeated for the next ξ value and the problem is solved line by line until $\xi = 1$ is reached. A convergence criterion based on the relative difference between the current and the previous iterations is employed. When this difference reaches 10^{-5}, the solution is assumed to have converged and the iterative process is terminated.

We have also examined the effect of the grid size $\Delta\eta$ and $\Delta\xi$, and the edge of the boundary layer η_∞ on the solution. The results presented here are independent of the grid size and η_∞ at least upto the fourth decimal place.

The numerical results presented here employed $\Delta\eta = 0.02$, $\Delta\xi = 0.005$, and $\eta_\infty = 8$.

5. Results and discussion

In order to validate our results, we have compared the surface shear stress ($f''(\xi,0)$) and the surface heat transfer ($-\theta'(\xi,0)$ or $1/\theta(\xi,0)$) for the prescribed surface temperature and heat flux when $\xi = 1$ with those of Ramachandran et al. [3]. Also for $\lambda = 0$ (no buoyancy force) we have compared our surface shear stress ($f''(\xi,0)$) with that of Williams and Rhyne [11]. The results are found to be in excellent agreement. The comparison is shown in Figs. 2–5.

The variation of the surface shear stress ($f''(\xi,0)$) with time $\xi(0 \leqslant \xi \leqslant 1)$ for the buoyancy assisting and opposing flows ($\lambda_1 = \pm 1$) and for the PST case with $Pr = 0.7$, 7, 20, 60, $n = 1$ (non-isothermal surface) is shown in Fig. 2. At the start of the motion ($\xi = 0$) the buoyancy force (λ_1) and the Prandtl number (Pr) have no effect on the surface shear stress ($f''(\xi,0)$) and these effects become pronounced with increasing time (ξ). The

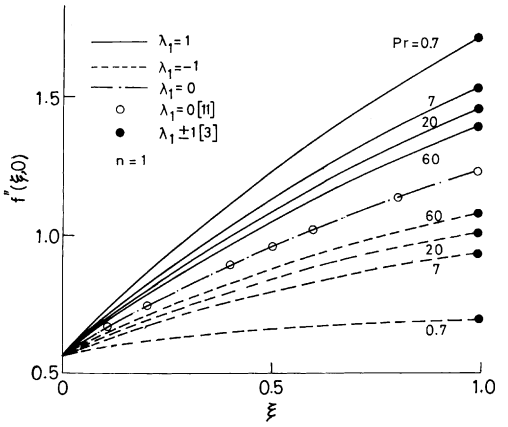

Fig. 2. Variation of the surface shear stress ($f''(\xi,0)$) with time ξ for the PST case when $\lambda_1 = \pm 1$, 0, $n = 1$, $Pr = 0.7$, 7, 20, 60.

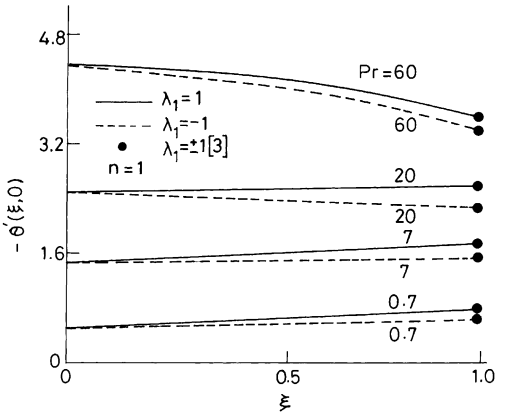

Fig. 3. Variation of the surface heat transfer ($-\theta'(\xi,0)$) with time ξ for the PST case when $\lambda_1 = \pm 1$, $n = 1$, $Pr = 0.7$, 7, 20, 60.

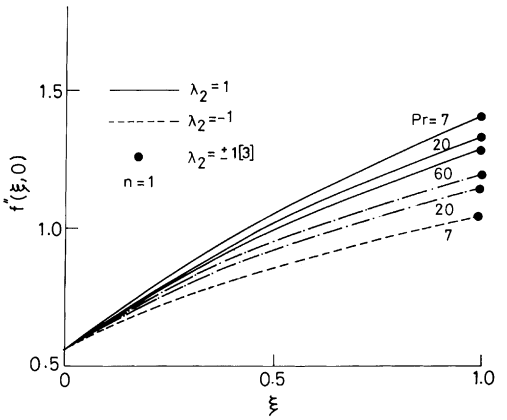

Fig. 4. Variation of the surface shear stress ($f''(\xi,0)$) with time ξ for PHF case when $\lambda_2 = \pm 1$, $n = 1$, $Pr = 7$, 20, 60.

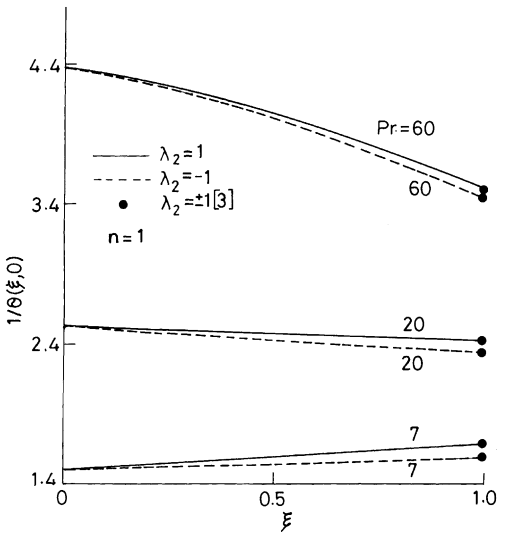

Fig. 5. Variation of the surface heat transfer $(1/\theta(\xi,0))$ with time ξ for PHF case when $\lambda_2 = \pm 1$, $n = 1$, $Pr = 7$, 20, 60.

steady-state is reached at $\xi = 1$ ($t^* \to \infty$). There is a smooth transition from the short-time solution to the long-time solution. Similar trend has been observed by Williams and Rhyne [11] for the forced flow on a wedge. The surface shear stress $(f''(\xi,0))$ increases with ξ, because, as mentioned earlier, the flow is dominated by the convective acceleration for large ξ. For buoyancy assisting flow ($\lambda = 1$), the effect of ξ becomes less pronounced with increasing Pr, but the opposite trend is observed for buoyancy opposing flow ($\lambda_1 = -1$). For buoyancy assisting flow ($\lambda_1 = 1$) and for $Pr = 0.7$, $f''(\xi,0)$ increases by about 202% as ξ increases from 0 to 1, but for buoyancy opposing flow ($\lambda_1 = -1$), it increases by about 22%. On the other hand for $Pr = 20$, $f''(\xi,0)$ increases by about 156% for $\lambda_1 = 1$ as ξ increases from 0 to 1, but for $\lambda = -1$ it increases by about 78%. For buoyancy assisting flow ($\lambda_1 = 1$) and for $\xi = 1$, $f''(\xi,0)$ decreases with increasing Prandtl number Pr. The reason for this trend is that the higher Prandtl number implies more viscous fluid which increases the boundary layer thickness and this causes reduction in the shear stress. For $\xi = \lambda_1 = n = 1$, $f''(\xi,0)$ decreases by about 23% as Pr increases from 0.7 to 60. For buoyancy opposing flow ($\lambda_1 = -1$), $f''(\xi,0)$ increases with Pr. Similar trend has been observed by Ramachandran et al. [3]. For $\xi = n = 1$, $\lambda_1 = -1$, $f''(\xi,0)$ increases by about 55% as Pr increases from 0.7 to 60. Also for a fixed Pr, $f''(\xi,0)$ increases with the buoyancy parameter λ_1 and this increase is more for the lower Prandtl number. This increase is caused by the enhancement in the velocity due to the assisting buoyancy force which acts like a favourable pressure gradient and the effect of buoyancy force is more pronounced for the lower Pr. When $\xi = n = 1$, $Pr = 0.7$, $f''(\xi,0)$ increases by about 145% as λ_1 increases from -1 to 1, but for $Pr = 0.7$ it increases by about 64%.

Fig. 3 presents the variation of the surface heat transfer $(-\theta'(\xi,0))$ with time $\xi (0 \leqslant \xi \leqslant 1)$ for buoyancy assisting and opposing flows ($\lambda_1 = \pm 1$) and for the PST case with $Pr = 0.7$, 7, 20, 60, $n = 1$. The surface heat transfer changes little with ξ except when Pr is large ($Pr = 60$). For this case $-\theta'(\xi,0)$ decreases by about 14% as ξ increases from 0 to 1. For a fixed time ξ, $-\theta'(\xi,0)$ increases significantly with Pr, because the higher Prandtl number fluid has a lower thermal conductivity which results in thinner thermal buoyancy layer and hence a higher heat transfer rate at the surface. At $\xi = 0$, $-\theta'(\xi,0)$ increases by about 700% as Pr increases from 0.7 to 60 and at $\xi = 1$ it is about 364%. Similar trend has been observed for buoyancy opposing flow ($\lambda_1 = -1$). Also for $\xi > 0$, heat transfer for the buoyancy opposing flow is less than that of the buoyancy assisting flow.

For PHF case the corresponding results for the surface shear stress $(f''(\xi,0)$ and the reciprocal of the surface temperature $(1/\theta(\xi,0))$, which represents the surface heat transfer for the PHF case, are presented in Figs. 4 and 5, respectively. Since these results are qualitatively similar to those of the PST case, they are not discussed here. For buoyancy assisting flow and for $\xi > 0$, the surface shear stress and the surface heat transfer for the PHF case are less than those of the PST case, but for the buoyancy opposing flow the reverse trend is observed. Similar trend is also observed by Ramchandran et al. [3] for the steady case ($\xi = 1$).

Fig. 6 displays the variation of the skin friction coefficient $(2^{-1}Re_x^{1/2}c_f)$ and the Nusselt number

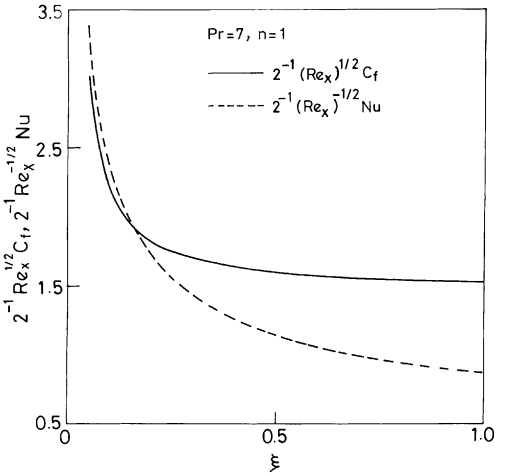

Fig. 6. Variation of the skin friction coefficient $(2^{-1}Re_x^{1/2}c_f)$ and the Nusselt number $(re_x^{1/2}Nu)$ with time ξ for the PST case when $\lambda_1 = \pm 1$, $Pr = 7$.

($Re_x^{-1/2}Nu$) with time ξ for the PST case when $Pr = 7$, $\lambda_1 = n = 1$. The corresponding results for the buoyancy opposing flow and for the PHF case are qualitatively similar to the above results. Hence they are not shown here. Due to the impulsive motion the skin friction and the heat transfer coefficients have large values for small time after the start of the motion and they decrease continuously and reach the steady-state values at $\xi = 1 (t^* \to \infty)$.

The variation of the surface shear stress ($f''(\xi,0)$) and the surface heat transfer ($-\theta'(\xi,0)$) with time ξ for the PST case when the buoyancy parameter $\lambda_1 = 0$, 5, 10, $Pr = 0.7$, $n = 1$ is shown in Fig. 7. The surface shear stress and the heat transfer increase with λ_1, because positive buoyancy force acts like favourable pressure gradient which accelerates the motion and reduces both momentum and thermal boundary layers. Hence both the surface shear stress and the surface heat transfer are increased. For $\xi = 0.5$, $Pr = 0.7$, $n = 1$, $f''(\xi,0)$ and $-\theta'(\xi,0)$ increase by about 265% and 46%, respectively, as λ_1 increases from 0 to 10. Fig. 7 also shows the surface heat transfer ($-\theta'(\xi,0)$) for $n = 0$ (isothermal surface), -0.5, $\lambda_1 = 10$, $Pr = 0.7$. For isothermal case, the heat transfer is found to be less (about 42%) than that of $n = 1$ (non-isothermal case). For $n = -0.5$, the time variation of the heat transfer is very small. The surface shear stress ($f''(\xi,0)$) is slightly higher (about 7.5%) than that of $n = 1$ when $\xi = 1$. Hence it is not shown in the figure. The reason for this trend is that for $n = 0$ the surface temperature difference ($T_w - T_\infty$) is less than that of $n = 1$. This results in lower heat transfer for $n = 0$ as compared to $n = 1$. Also, for gases ($\mu \propto T$) reduction in surface temperature causes thinner boundary layer which in turn increases the surface shear stress.

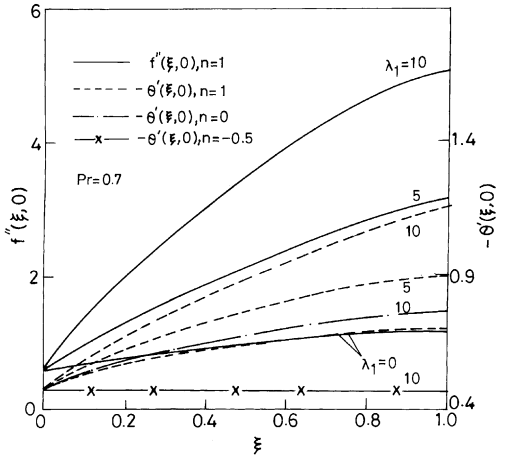

Fig. 7. Variation of the surface shear stress ($f''(\xi,0)$) with the surface heat transfer ($1/\theta(\xi,0)$) with time ξ for PST case when $\lambda_1 = 0$, 5, 10, $Pr = 0.7$, $n = -0.5$, 0, 1.0.

6. Conclusions

The surface shear stress and heat transfer, in general, increase with time and there is a smooth transition from the small-time solution to the large-time solution. The surface shear stress and heat transfer for buoyancy assisting flow are more than those of the buoyancy opposing flow. The surface heat transfer increases with increasing Prandtl number, but the surface shear stress decreases for the buoyancy assisting flow and increases for the buoyancy opposing flow. For buoyancy assisting flow, the surface shear stress and heat transfer for the prescribed surface heat flux are slightly less than those of the prescribed surface temperature, but for the buoyancy opposing flow the reverse trend is observed. The surface heat transfer can considerably be reduced by using a lower Prandtl number fluid. It can also be reduced by imposing the buoyancy force in the opposite direction to that of the forced flow or by maintaining uniform temperature or heat flux on the surface.

References

[1] K. Hiemenz, Die Grenzschicht an einem in den gleich formigen FlussigKeitsstrom eingetacuhten geraden kreßzylinder, Dinglers Polytech. J. 326 (1911) 321–324.

[2] E.R.G. Eckert, Die Berechnung des Wärmeübergangs in der laminaren Grenzschicht umströmter Köper, VDI Forschung.

[3] N. Ramachandran, T.S. Chen, B.F. Armaly, Mixed convection in stagnation flows adjacent to vertical surface, J. Heat Transfer 110 (1988) 173–177.

[4] K. Stewartson, On the impulsive motion of a flat plate in a viscous fluid, Part 1, Quart. J. Mech. Appl. Math. 4 (1951) 182–198.

[5] K. Stewartson, On the impulsive motion of a flat plate in a viscous fluid, Part 2, Quart. J. Mech. Appl. Math. 22 (1973) 143–152.

[6] M.G. Hall, The boundary layer over an impulsively started flat plate, Proc. R. Soc. 310A (1969) 401–414.

[7] S.C.R. Dennis, The motion of a viscous fluid past an impulsively started semi-infinite flat plate, J. Inst. Math. Its Appl. 10 (1972) 105–117.

[8] C.B. Watkins, Heat transfer in the boundary layer over an impulsively started flat plate, J. Heat Transfer 97 (1975) 482–484.

[9] S.H. Smith, The impulsive motion of a wedge in a viscous fluid, Z. Angew. Math. Phys. 18 (1967) 508–522.

[10] K. Nanbu, Unsteady Falkner–Skan flow, Z. Angew. Math. Phys. 22 (1971) 1167–1172.

[11] J.C. Williams, T.H. Rhyne, Boundary layer development on a wedge impulsively set into motion, SIAM J. Appl. Math. 38 (1980) 215–224.

[12] M.C. Ece, An initial boundary layer flow past a translating and spinning rotational symmetric body, J. Eng. Math. 26 (1992) 415–428.

[13] A. Ozturk, M.C. Ece, Unsteady forced convection heat transfer from a translating and spinning body, J. Energy Resour. Technol. 117 (1995) 318–323.
[14] M. Kumari, Development of flow and heat transfer on a wedge with a magnetic field, Arch. Mech. 49 (1997) 977–990.
[15] S.N. Brown, N. Riley, Flow past a suddenly heated vertical plate, J. Fluid Mech. 59 (1973) 225–237.
[16] D.B. Ingham, Flow past a suddenly heated vertical plate, Proc. R. Soc. 402A (1985) 109–134.
[17] N. Amin, N. Riley, Mixed convection at a stagnation point, Quart. J. Mech. Appl. Math. 48 (1995) 111–121.
[18] F.G. Blottner, Finite-difference methods of solution of the boundary layer equations, AIAA J. 8 (1970) 193–205.
[19] M. Abramowitz, I.A. Stegun, in: Handbook of Mathematical Functions, vol. 55, Providence, National Bureau of Standard, Am. Math. Soc., 1972.